Atmos. Chem. Phys. Discuss., doi:10.5194/acp-2016-672, 2016
Manuscript under review for journal Atmos. Chem. Phys.
Published: 4 August 2016

Atmospheric Chemistry and Physics Discussions

The effect of adding hydroxyl functional groups and increasing molar mass on the viscosity of organics relevant to secondary organic aerosols

James W. Grayson[1], Mijung Song[1*], Erin Evoy[1], Mary Alice Upshur[2], Marzieh Ebrahimi[3], Franz M. Geiger[2], Regan J. Thomson[2], and Allan K. Bertram[1]

[1]Department of Chemistry, University of British Columbia, 2036 Main Mall, Vancouver, BC, V6T 1Z1, Canada
[2]Department of Chemistry, Northwestern University, 2145 Sheridan Road, Evanston, Illinois, 60208, United States
[3]Department of Chemical and Biological Engineering, University of British Columbia, 2360 East Mall, Vancouver, BC, V6T 1Z3, Canada
[*]Now at: Department of Earth and Environmental Sciences, Chonbuk National University, Jeollabuk-do, Republic of Korea

Correspondence to: Allan Bertram (bertram@chem.ubc.ca)

Abstract. In the following we determine the viscosity of four polyols (2-methyl-1,4-butanediol, 1,2,3-butanetriol, 2-methyl-1,2,3,4-butanetetrol, and 1,2,3,4-butanetetrol) and three saccharides (glucose, raffinose and maltohexaose) mixed with water. The polyol studies were carried out to quantify the relationship between viscosity and the number of hydroxyl (OH) functional groups in organic molecules, whilst the saccharide studies were carried out to quantify the relationship between viscosity and molar mass for highly oxidised organic molecules. Each of the polyols was of viscosity $\leq$6.5e2 Pa s, and a linear relationship was observed between $\log_{10}$(viscosity) and the number of OH functional groups (R^2 $\geq$0.99) for several carbon backbones. The linear relationship suggests that viscosity increases by 1-2 orders of magnitude with the addition of an OH functional group to a carbon backbone. For saccharide-water particles, studies at 28 % RH show an increase in viscosity of 3.6-6.0 orders of magnitude as the molar mass of the saccharide is increased from 180 to 342 g mol^{-1}, and studies at 77-80 % RH, show an increase in viscosity 4.6-6.2 orders of magnitude as molar mass increases from 180 to 991 g mol^{-1}. These results suggest oligomerisation of highly oxidised compounds in atmospheric SOM could lead to large increases in viscosity, and may be at least partially responsible for the high viscosities that are observed in some SOM. Finally, two quantitative structure-property relationship models were used to predict the viscosity of the four polyols studied. The model of Sastri and Rao (1992) was determined to over-predict the viscosity of each of the polyols, with the over-prediction being up to 19 orders of magnitude. The viscosities predicted by the model of Marrero-Morejón and Pardillo-Fontdevila (2000) were much closer to the experimental values, with no values differing by more than 1.3 orders of magnitude.

1 Introduction

Secondary organic material (SOM) is formed in the atmosphere through the oxidation of volatile organic compounds emitted from the Earth's surface by a range of natural and anthropogenic sources (Hallquist et al., 2009). SOM is estimated to account for 30-70 % of the mass of submicrometer atmospheric particulate matter in most regions of the atmosphere (Kanakidou

Atmos. Chem. Phys. Discuss., doi:10.5194/acp-2016-672, 2016
Manuscript under review for journal Atmos. Chem. Phys.
Published: 4 August 2016

Atmospheric Chemistry and Physics Discussions

et al., 2005), and directly and indirectly affects the Earth's climate (Stocker et al., 2013), as well as affecting human health (Baltensperger et al., 2008).

Despite its importance, many of the physical properties of SOM, such as its viscosity, remain poorly understood. Information on the viscosity of SOM may be important for several reasons. For example, viscosity may be needed for predicting the mass and size distribution of SOM particles in the atmosphere (Shiraiwa and Seinfeld, 2012; Shiraiwa et al., 2013; Zaveri et al., 2014). Viscosity information may also be needed for predicting heterogeneous chemistry, photochemistry and the long range transport of pollution (Berkemeier et al., 2016; Hinks et al., 2016; Houle et al., 2015; Kuwata and Martin, 2012; Lignell et al., 2014; Shiraiwa et al., 2011; Steimer et al., 2015; Wang et al., 2015; Zelenyuk et al., 2012; Zhou et al., 2012, 2013). Phase transitions and hygroscopic properties of SOM may also be susceptible to particle viscosity (Bodsworth et al., 2010; Bones et al., 2012; Hawkins et al., 2014; Ignatius et al., 2015; Ladino et al., 2014; Lienhard et al., 2015; Lu et al., 2014; Murray and Bertram, 2008; Price et al., 2014, 2015; Schill et al., 2014; Song et al., 2012; Tong et al., 2011; Wang et al., 2012; Wilson et al., 2012). Nevertheless, our understanding of the viscosity of SOM particles remains limited. Methods for predicting the viscosity of SOM from other properties of SOM, such as molar mass, and the organic functional groups, may be especially beneficial.

In the following we determine the viscosity of four polyols (2-methyl-1,4-butanediol, 1,2,3-butanetriol, 1,2,3,4-butanetetrol and 2-methyl-1,2,3,4-butanetetrol). Properties and structures of these polyols are shown in Table 1 and Figure 1. The viscosity of polyols were measured to quantify the relationship between viscosity and the number of hydroxyl (OH) functional groups in organic molecules. Polyols were also chosen for study due to their atmospheric importance, as, for example, tetraols have been observed in ambient particles and particles generated in environmental chambers (Claeys et al., 2004; Edney et al., 2005; Surratt et al., 2006, 2010).

In addition to polyols, we determined the viscosity of three saccharides (glucose, raffinose and maltohexaose). The saccharides were studied mixed with water. Properties and structures of these saccharides are also shown in Table 1 and Figure 1. Although the viscosity of sucrose has been measured over a wide range of relative humidities (RH) (Först et al., 2002; Grayson et al., 2015; Power et al., 2013; Quintas et al., 2006; Swindells et al., 1958; Telis et al., 2007) similar studies for glucose, maltohexaose and raffinose have yet to be carried out. The saccharides were studied to quantify the relationship between viscosity and molar mass for highly oxidised organic molecules. By studying these saccharides, the relationship between viscosity and molar mass was isolated while the O:C ratio and types of functional groups in the molecule remain largely unchanged. Saccharides including levoglucosan, glucose, xylose, sucrose, and maltose have been observed in wood smoke (Nolte et al., 2001), and saccharides may be responsible for the majority of the organic mass in ambient submicron particles in remote marine boundary layers (Russell et al., 2010).

The average O:C ratio of SOM has been determined to range from 0.3-1.1 (Chen et al., 2011; Jimenez et al., 2009; Lambe et al., 2015). The polyols studied ranged in O:C from 0.4-1.0 (Table 1), similar to that of SOM, and the saccharides studied have an O:C of 0.86-1.0 (Table 1), which is similar to that of the more highly oxidised components of SOM.

In addition to measuring the viscosity of the polyol compounds, we compared the measured viscosities of these compounds, as well as literature viscosity values for related alkanes, alcohols, and polyols, with predictions from two structure activity models (Marrero-Morejón and Pardillo-Fontdevila, 2000; Sastri and Rao, 1992). These two models have been derived and val-

Atmos. Chem. Phys. Discuss., doi:10.5194/acp-2016-672, 2016
Manuscript under review for journal Atmos. Chem. Phys.
Published: 4 August 2016

Atmospheric Chemistry and Physics Discussions

idated using organic compounds with viscosities <100 Pa s. As such, their applicability to organic compounds with viscosities >100 Pa s is uncertain.

2 Experimental

2.1 Viscosity measurements

Three different techniques were used to determine viscosity: a rotational rheometer, a bead mobility technique and a poke-and-flow technique. The technique used for each compound is reported in Table 4. In addition, the techniques are described in more detail below.

2.2 Rotational rheometry

The rotational rheometer has been described in detail previously (Collyer and Clegg, 1988). For measurements, a commercial rotational rheometer with a cup and bob fixture was used (MCR 501, Anton Paar, Austria, as described in Behzadfar and Hatzikiriakos (2014)). The amount of material needed for the measurements was $\geq$5 mL. A temperature-controlled sample compartment on the rheometer was used to perform measurements at 295 K, using a shear rate ranging from 1-100 s^{-1}.

2.3 Bead mobility technique

The bead-mobility technique has been described in detail previously (Renbaum-Wolff et al., 2013b). Briefly, an aqueous solution of the material was nebulized onto a hydrophobic substrate, forming super-micron sized particles (30-70 μm in diameter) on the hydrophobic substrate. A solution containing micron-sized melamine beads was subsequently nebulised over the top of the substrate, resulting in the incorporation of the melamine beads into the particles. The substrate was then fixed inside a flow cell, and the flow cell subsequently mounted to an optical microscope. Particles were allowed to equilibrate at a given relative humidity (RH) using a humidity-controlled flow of N_2 gas through the flow cell, which also imparts a shear stress on the surface of the particles. This shear stress caused the material in the particle to circulate in well-defined patterns. The speeds at which beads were observed to circulate within a particle were determined from images recorded during the experiments, and the bead speeds were converted to viscosities using a calibration curve, which was created using sucrose-water and glycerol-water particles, two systems with well-constrained viscosities. Experiments were performed at room temperature (294-295 K).

2.4 Poke-and-flow technique

The poke-and-flow technique has been described in detail previously (Grayson et al., 2015; Renbaum-Wolff et al., 2013a). The technique builds on the qualitative approach described by Murray et al. (2012). An aqueous solution of the material was nebulized onto a hydrophobic substrate, forming super-micron sized particles (30-70 μm in diameter) on the hydrophobic substrate. The substrate was fixed inside a flow cell, and the flow cell subsequently mounted to an optical microscope. Particles were allowed to equilibrate at a given RH and room temperature (294-295 K). Then the particles were poked using a needle

Atmos. Chem. Phys. Discuss., doi:10.5194/acp-2016-672, 2016
Manuscript under review for journal Atmos. Chem. Phys.
Published: 4 August 2016

Atmospheric Chemistry and Physics Discussions

attached to a micromanipulator. If the viscosity of the material was low, the action of poking the particles with a needle caused the material to form a half torus geometry. When the needle was removed, the material flowed and reformed the energetically favourable hemispherical morphology. Figure 2, Panel a, provides an example of images recorded during an experiment where the material flowed and reformed the hemispherical geometry after poking. From images recorded during the experiments, the experimental flow time, τ_{exp}, flow, was determined, where τ_{exp}, flow is the time taken for the diameter of the hole after poking to decrease to half of its original value.

If the viscosity of the material was high, the action of poking the particles with a needle caused the material to crack with no flow being detected over the period of several hours. See Figure 2, Panel b, for an example of images recorded during an experiment where the material cracked after poking and did not flow over the period of several hours after cracking.

To determine viscosities from the poke-and-flow experiments, the behaviours observed in the experiments and described above were subsequently simulated using a multiphysics program (COMSOL multiphysics). For experiments where flow was observed, a half-torus geometry was used in the simulations with dimensions based on the dimensions observed in experiments. For more details of the simulations used when flow was observed see Grayson et al. (2015). Input to the simulations included the slip length (which describes the interaction between the material and the hydrophobic glass slide), the surface tension of the material, the contact angle between the material and hydrophobic glass surface and the density of the material. Physical parameters used in the simulations where flow was observed are listed in Table 2.

For experiments where cracking was observed, lower limits to the viscosity were determined using the COMSOL Multiphysics simulations. In this case, the geometry used in the simulations was a quarter-sphere geometry, with one flat surface in contact with a solid substrate, which represents the hydrophobic glass surface (Renbaum-Wolff et al., 2013a). In these simulations the viscosity of the material was varied until the sharp edge at the top of the quarter-sphere moved by 0.5 μm over the experimental time. A movement of 0.5 μm would be discernible in the microscope experiments, and hence the simulated viscosity represents a lower limit to the viscosity, since no movement was observed in the experiments. The physical properties used for the cases where particles were observed to crack and no flow was observed over the course of the experiment are given in Table 3. Additional details for these types of simulations are given in Renbaum-Wolff et al. (2013a).

2.5 Compounds studied

2-Methyl-1,4-butanediol ($\geq$97 % purity), 1,2,3-butanetriol ($\geq$90 % purity), 1,2,3,4-butanetetrol ($\geq$99 % purity), β-D-Glucose ($\geq$99.5 % purity), raffinose ($\geq$98 % purity), and maltohexaose ($\geq$65 % purity) were obtained from Sigma-Aldrich. *Syn*-2-methyl-1,2,3,4-butanetetrol was prepared in diastereomerically pure form starting from protected *cis*-2-methylbut-2-ene-1,4-diol based on the procedure described in Ebben et al. (2014). The purity of the tetraol was determined based on ^{1}H and ^{13}C NMR spectroscopy. In order to test stability, solutions containing 100 mM of the tetraol in 1 M $(NH_4)_2SO_4$ and D_2O were stirred at room temperature for one week and monitored by NMR spectroscopy. No changes in composition were observed during this time. While 2-Methyl-1,2,3,4-butanetetraol also exists as the anti diastereomer, preliminary viscosity measurements at room temperature using a method similar to a Cannon-Fenske viscometer indicated that the viscosities of the two tetraol

Atmos. Chem. Phys. Discuss., doi:10.5194/acp-2016-672, 2016
Manuscript under review for journal Atmos. Chem. Phys.
Published: 4 August 2016

Atmospheric Chemistry and Physics Discussions

diastereomers were identical within error (Upshur et al., 2014). As a result, only the syn diastereomer was analyzed in this study.

The RHs at which viscosities were measured for each of the compounds are detailed in Table 4. Glucose was studied only at 28 % RH as viscosity measurements at RH values >28 % have been reported in the literature and at <28 % RH the particles stuck to the needle and were removed from the substrate, meaning their viscosity could not be determined. Raffinose particles were studied at RH values ranging from 40 to 85 %. At 40 % the particles cracked when poked, and did not flow on a laboratory timescale. The same results were expected as lower RH values, and so lower RH values were not covered. Maltohexaose particles were studied at RH values ranging from 50 to 80 %. As the particles cracked and did not flow at either 60 % RH or 50 % RH, experiments were not carried out at lower RH values. The polyols were only studied under dry conditions.

2.6 Predictions of viscosity using quantitative structure-property relationship models

Two quantitative structure-property relationship (QSPR) models were used to estimate the viscosity of the four polyols studied here. QSPR models relate physical, chemical, or physicochemical properties of compounds to their structures. The first QSPR model used, which was developed by Sastri and Rao (1992), estimates the viscosity of a compound at a given temperature (295 K was used here) based on its vapour pressure at that temperature, along with the number and type of functional groups in the molecule. Where available, literature vapour pressure values at 295 K (Cai et al., 2015; Cammenga et al., 1977; Green and Perry, 2007; Verevkin, 2004) were used to predict the viscosities of the alkanes, alcohols, and the polyols. Experimental measurements of the vapour pressure of the four polyols of main focus in this study (1,2,3-butanetriol, 1,2,3,4-butanetetrol, 2-methyl-1,4-butanediol, and 2-methyl-1,2,3,4-butanetetrol) were not available, and so their vapour pressures were estimated at 295 K using the three QSPR models employed by the E-AIM vapour pressure calculator ($http://www.aim.env.uea.ac.uk/aim/ddbst/pcalc_main.php$). Each of the QSPR models used to estimate vapour pressure is based on the boiling point of the molecule along with group contributions from the functional groups present in its structure. The first model uses the method of Nannoolal et al. (2004) to predict the boiling point, and the method of Moller et al. (2008) to predict vapour pressure, the second uses the method of Nannoolal et al. (2004) to predict the boiling point and the method of Nannoolal et al. (2008) to predict vapour pressure, and the third uses the method of Stein and Brown (1994) to predict the boiling point and the method of Myrdal and Yalkowsky (1997) to predict vapour pressure. The three models each gave rise to a different estimation of the vapour pressure of each polyol, and the lower and upper estimations of vapour pressure were used to estimate lower and upper limits of viscosity.

The second QSPR model used to predict viscosity was proposed by Marrero-Morejón and Pardillo-Fontdevila (2000) and estimates a compound's viscosity only at 293 K based on its molar mass and the type and number of bonds and functional groups within the molecule. Although 293 K is slightly lower than the temperature at which viscosities measurements were made in this study, the small difference in temperature between the model and experiments (1-2 K) should not lead to large discrepancies.

Atmos. Chem. Phys. Discuss., doi:10.5194/acp-2016-672, 2016
Manuscript under review for journal Atmos. Chem. Phys.
Published: 4 August 2016

Atmospheric Chemistry and Physics Discussions

3 Results and discussion

3.1 Viscosity of polyols

The viscosities of four different polyols, containing two to four hydroxyl (OH) functional groups, were determined experimentally using the bead-mobility and the rotational rheometer techniques. The measured viscosities are summarised in Table 4. The mean viscosities of the polyols range from 1.3e-1 to 2.3e2 Pa s, with the tetraols having the highest viscosities. For reference, these viscosities lie between that of water (1e-3 Pa s) and that of peanut butter (1e3 Pa s), whilst the viscosity of honey is approximately 1e1 Pa s (Koop et al., 2011).

The viscosities detailed in Table 4 are also plotted in Figure 3 (open symbols) as a function of the number of OH functional groups in the molecule. Each panel only includes molecules comprised of a specific carbon backbone in order to isolate the effect of adding an OH functional group to a carbon backbone. Panels (a) and (b), correspond to a linear C4 and a branched C5 carbon-backbone, respectively. Also included in Figure 3 (filled symbols) are literature viscosities for compounds with a linear C4 and branched C5 carbon-backbone and having zero to two OH functional groups. Values reported in Figure 3 correspond to a temperature of 294-295 K, the temperature at which measurements were made here. Literature viscosities are determined at 295 K using a polynomial interpolation of available temperature dependent values of $\log_{10}$(viscosity) (Czechowski et al., 2004; Haynes, 2015; Jarosiewicz et al., 2004; Viswanath et al., 2007).

Both of the panels in Figure 3 exhibit a clear relationship between $\log_{10}$(viscosity) and the number of OH functional groups in the compound. Included on each panel is a linear fit to the data, and each line has a coefficient of determination (R^2) $\geq$0.99. The slopes of the fits were 1.32 and 1.51 for the linear C4 and branched C5 backbones, respectively.

In Figure 4, using literature viscosity data, we show that a linear relationship also exists between $\log_{10}$(viscosity) and the number of OH functional groups for molecules with a linear C3 and a linear C6 carbon backbone and having zero to three OH functional groups. Again, literature viscosities are determined at 295 K using a polynomial interpolation of available temperature dependent values of $\log_{10}$(viscosity) (Czechowski et al., 2004; Haynes, 2015; Sheely, 1932; Sigma-Aldrich, 1996). The slopes of the fits for the C3 and C6 backgrounds are 1.38 and 1.27.

Based on Figure 3 and Figure 4, oxidation reactions in the atmosphere that lead to the incorporation of a single OH functional group in a compound would be expected to form a product with a viscosity of one to two orders of magnitude greater than that of its precursor, assuming no fragmentation.

3.2 Viscosity of saccharides

Mixtures of a saccharide and water were studied using the bead-mobility and poke-and-flow techniques across a range of RHs. The simulated viscosities for each of the saccharide particles are grouped by RH and summarised in Table 4, and shown in Figure 5(a). Also included in Figure 5(a) are literature data for the viscosity of glucose-water mixtures at $\geq$75 % RH (Achard et al., 1992; Barbosa-Canovas, 2007; Haynes, 2015) and sucrose-water mixtures for RH values $\geq$ 25 % RH (Först et al., 2002; Power et al., 2013; Quintas et al., 2006; Swindells et al., 1958; Telis et al., 2007). The viscosity of each of the saccharides was observed to increase as RH is decreased, with the viscosity at 28 % RH at least four orders of magnitude greater than at

Atmos. Chem. Phys. Discuss., doi:10.5194/acp-2016-672, 2016
Manuscript under review for journal Atmos. Chem. Phys.
Published: 4 August 2016

Atmospheric Chemistry and Physics Discussions

78 % RH. This inverse relationship between viscosity and RH is due to the behaviour of water as a plasticiser (a component that reduces the viscosity of a solution) and the greater water content in particles at higher relative humidities (Renbaum-Wolff et al., 2013a).

Figure 5(b) is a plot of viscosity vs. molar mass of the saccharides at three RHs for saccharide-water mixtures. At 28 % RH, the viscosity increased by 3.6-6.0 orders of magnitude as molar mass of the saccharide increased from 180 to 342 g mol^{-1}, and at 77-80 % RH the viscosity increased by 4.6-6.2 orders of magnitude as the molar mass of the saccharide increased from 180 to 991 g mol^{-1}. These observations are consistent with prior studies that suggest viscosity and molar mass are related through a power function (Hiemenz and Lodge, 2007; Pachaiyappan et al., 1967). These observations are also consistent with prior studies that have shown a relationship between glass transition temperature and molar mass (Koop et al., 2011; Zobrist et al., 2008) and a relationship between bounce of particles off of surfaces and molar mass (Li et al., 2015; Saukko et al., 2012).

3.3 Comparison of measured and predicted viscosities

As discussed in Section 2.6, two QSPR models have been used to predict the viscosities of the polyols studied here. The first QSPR model (Sastri and Rao, 1992) relates viscosity to the molecular structure and vapor pressure of a compound, whilst the second QSPR model (Marrero-Morejón and Pardillo-Fontdevila, 2000) relates viscosity to the molecular structure and molar mass of a compound.

Figure 6 is a plot of measured vs. predicted viscosity for the polyols measured here. The QSPR model of Sastri and Rao (1992) (Figure 6(a)) over-predicts the viscosity of 2-methyl-1,4-butanediol by 2.7-3.0 orders of magnitude, the viscosity of 1,2,3-butanetriol by 6.5-7.8 orders of magnitude, the viscosity of 2-methyl-1,2,3,4-butanetetrol by 14.7-18.7 orders of magnitude, and the viscosity of 1,2,3,4-butanetetrol by 7.2-10.3 orders of magnitude.

Shown in Figure 6(b) are predicted viscosities using the QSPR model of Marrero-Morejón and Pardillo-Fontdevila (2000). The model provides more accurate predictions than that of Sastri and Rao (1992), with the predicted viscosities of 2-methyl-1,4-butanediol and 1,2,3,4-butanetetrol being in agreement with those predicted, while the predicted viscosity of 1,2,3-butanetriol is lower than the measured viscosity by 0.1-0.2 orders of magnitude, and the predicted viscosity of 2-methyl-1,2,3,4-butanetetrol is lower than the measured viscosity by 0.6-1.3 orders of magnitude.

Shown in Figure 7 is a comparison of measured and predicted viscosities for all the alkanes, alcohols and polyols shown in Figure 3 and Figure 4. In Figure 7 the number of OH functional groups in each molecule are identified using different symbols. The QSPR model of Sastri and Rao (1992) predicts well the viscosities of molecules containing zero and one OH functional groups, but the model increasingly over-predicts the viscosity as the number of OH functional groups increases above one. On the other hand, the QSPR model of Marrero-Morejón and Pardillo-Fontdevila (2000) predicts well the literature viscosity values of molecules containing up to two OH functional groups, and the viscosities of 2-methyl-1,4-butanediol and 1,2,3,4-butanetetrol. The model of Marrero-Morejón and Pardillo-Fontdevila (2000) under-predicts the viscosities of 1,2,3-butanetriol and 2-methyl-1,2,3,4-butanetetrol by 0.1-0.2 and 0.6-1.3 orders of magnitude, respectively. This under-prediction may be explained in part by the lower temperature used in the model (293 K) compared to the experimental temperature of

Atmos. Chem. Phys. Discuss., doi:10.5194/acp-2016-672, 2016
Manuscript under review for journal Atmos. Chem. Phys.
Published: 4 August 2016

294-295 K used here. If an Arrhenius type relationship exists between viscosity and temperature for these compounds, an increase in temperature of 2 K would be expected to cause viscosity to decrease by 0.1 orders of magnitude.

4 Atmospheric implications

An estimated 500-750 Tg of isoprene is emitted annually from the Earth's surface (Guenther et al., 2006). Once in the atmosphere, isoprene molecules react predominantly with hydroxyl (OH) radicals (Worton et al., 2013), leading to products containing oxygen functional group(s). Previous characterisation studies of SOM produced via the oxidation of isoprene by OH radicals have identified the presence of triols and tetraols (Claeys et al., 2004; Edney et al., 2005), including 2-methyl-1,2,3,4-butanetetrol, which has been studied here. Recently, Song et al. (2015) measured the viscosity of SOM produced via the oxidation of isoprene in the absence of NO_x, and determined it to range between 2e4 and 4e6 Pa s at <1 % RH. The viscosity of 2-methyl-1,2,3,4-butanetetrol has been measured here to be 2.3e2 Pa s (95 % confidence limits of 1.4e2-6.5e2 Pa s), which implies there are individual components in the SOM studied by Song et al. with higher viscosity than 2-methyl-1,2,3,4-butanetetrol.

The results from the experiments with polyols, along with literature data for alkanes, alcohols, and polyols suggest that adding a hydroxyl (OH) functional group to a carbon back-bone can increase the viscosity of the organic compound by 1-2 orders of magnitude. These results may be useful for estimating the viscosity of some components of SOM.

The results with the saccharides illustrate the strong dependence of molar mass on the viscosity of highly oxidised organic compounds. Oligomerisation reactions are known to occur in secondary organic aerosol, and efficiently increase the molar mass of a compound whilst keeping its O:C ratio roughly constant. Oligomers have been estimated to account for up to 50 % of the mass of SOM (Baltensperger et al., 2005; Gao et al., 2004; Hallquist et al., 2009; Tolocka et al., 2006). The formation of oligomer products may proceed via a mechanism, such as dehydration (Muller et al., 2009) or the elimination of oxygen or carbon dioxide (Zhang et al., 2015). Consistent with previous suggestions (Kidd et al., 2014; Virtanen et al., 2010), our results with saccharides suggest that these types of reactions may play an important role in producing the high viscosities observed in SOM (Booth et al., 2014; Grayson et al., 2016; Pajunoja et al., 2014; Renbaum-Wolff et al., 2013a; Song et al., 2015; Zhang et al., 2015).

Two QSPR models were tested for their ability to predict the viscosity of alkanes, alcohols and polyols. The model of Sastri and Rao (1992) over-predicted the viscosities of compounds containing multiple oxygen-containing functional groups by up to 19 orders of magnitude and hence this model, in the current form, is not recommended for predicting the viscosity of components of SOM. On the other hand the model of Marrero-Morejón and Pardillo-Fontdevila (2000) shows reasonably good agreement with measured viscosities for alkanes, alcohols, and polyols. As such, this model shows potential for predicting the viscosity of SOM components. However, only a limited number of organic functional groups are included in the model. Some of the functional groups observed in extremely low volatility SOM, such as hydroperoxides, are not currently incorporated into the model. Expansion of the model by Marero-Morejón and Pardillo-Fortdevila to include these functional groups would be beneficial.

Atmos. Chem. Phys. Discuss., doi:10.5194/acp-2016-672, 2016
Manuscript under review for journal Atmos. Chem. Phys.
Published: 4 August 2016

Acknowledgements. This work was supported by the Natural Sciences and Engineering Research Council of Canada. R.J.T. and F.M.G. gratefully acknowledge support from the National Science Foundation (CHE 1212692). M.A.U. gratefully acknowledges support from a National Aeronautics and Space Administration Earth and Space (NASA ESS) Fellowship and a National Science Foundation (NSF) Graduate Research Fellowship (NSF GRFP).

Atmos. Chem. Phys. Discuss., doi:10.5194/acp-2016-672, 2016
Manuscript under review for journal Atmos. Chem. Phys.
Published: 4 August 2016

Atmospheric Chemistry and Physics Discussions

References

Achard, C., Dussap, C. G., and Gros, J.-B.: Prédiction de l'activité de l'eau, des températures d'ébullition et de congélation de solutions aqueuses de sucres par un modèle UNIFAC, Industries alimentaires et agricoles, 109, 93–101, 1992.

Baltensperger, U., Kalberer, M., Dommen, J., Paulsen, D., Alfarra, M. R., Coe, H., Fisseha, R., Gascho, A., Gysel, M., Nyeki, S., Sax, M., Steinbacher, M., Prevot, a. S. H., Sjögren, S., Weingartner, E., and Zenobi, R.: Secondary organic aerosols from anthropogenic and biogenic precursors., Faraday discussions, 130, 265–278, doi:10.1039/b417367h, 2005.

Baltensperger, U., Dommen, J., Alfarra, M. R., Duplissy, J., Gaeggler, K., Metzger, A., Facchini, M. C., Decesari, S., Finessi, E., Reinnig, C., Schott, M., Warnke, J., Hoffmann, T., Klatzer, B., Puxbaum, H., Geiser, M., Savi, M., Lang, D., Kalberer, M., and Geiser, T.: Combined determination of the chemical composition and of health effects of secondary organic aerosols: The POLYSOA project, Journal of Aerosol Medicine and Pulmonary Delivery, 21, 145–154, doi:10.1089/jamp.2007.0655, 2008.

Barbosa-Canovas, G. V.: Water activity in foods: Fundamentals and applications, Wiley-Blackwell, Hoboken, NJ, 2007.

Baudry, J., Charlaix, E., Tonck, A., and Mazuyer, D.: Experimental evidence for a large slip effect at a nonwetting fluid - solid interface, Langmuir, 17, 5232–5236, doi:10.1021/la0009994, 2001.

Behzadfar, E. and Hatzikiriakos, S. G.: Rheology of bitumen: Effects of temperature, pressure, CO2 concentration and shear rate, Fuel, 116, 578–587, doi:10.1016/j.fuel.2013.08.024, 2014.

Berkemeier, T., Steimer, S. S., Krieger, U. K., Peter, T., Pöschl, U., Ammann, M., and Shiraiwa, M.: Ozone uptake on glassy, semi-solid and liquid organic matter and the role of reactive oxygen intermediates in atmospheric aerosol chemistry, Phys. Chem. Chem. Phys., 18, 12 662–12 674, doi:10.1039/C6CP00634E, 2016.

Bodsworth, A., Zobrist, B., and Bertram, A. K.: Inhibition of efflorescence in mixed organic-inorganic particles at temperatures less than 250 K., Physical chemistry chemical physics : PCCP, 12, 12 259–12 266, doi:10.1039/c0cp00572j, 2010.

Bones, D. L., Reid, J. P., Lienhard, D. M., and Krieger, U. K.: Comparing the mechanism of water condensation and evaporation in glassy aerosol, Proceedings of the National Academy of Sciences of the United States of America, 109, 11 613–11 618, doi:10.1073/pnas.1200691109, 2012.

Booth, A. M., Murphy, B., Riipinen, I., Percival, C. J., and Topping, D. O.: Connecting bulk viscosity measurements to kinetic limitations on attaining equilibrium for a model aerosol composition, Environmental Science and Technology, 48, 9298–9305, doi:10.1021/es501705c, 2014.

Cai, C., Stewart, D. J., Reid, J. P., Zhang, Y. H., Ohm, P., Dutcher, C. S., and Clegg, S. L.: Organic component vapor pressures and hygroscopicities of aqueous aerosol measured by optical tweezers, Journal of Physical Chemistry A, 119, 704–718, doi:10.1021/jp510525r, 2015.

Cammenga, H. K., Schulze, F. W., and Theuerl, W.: Vapor pressure and evaporation coefficient of glycerol, Journal of Chemical and Engineering Data, 22, 131–134, doi:10.1021/je60073a004, 1977.

Chen, Q., Liu, Y., Donahue, N. M., Shilling, J. E., and Martin, S. T.: Particle-phase chemistry of secondary organic material: Modeled compared to measured O:C and H:C Elemental ratios provide constraints, Environmental Science and Technology, 45, 4763–4770, doi:10.1021/es104398s, 2011.

Cheng, J. T. and Giordano, N.: Fluid flow through nanometer-scale channels, Physical Review E - Statistical, Nonlinear, and Soft Matter Physics, 65, 031 206, doi:10.1103/PhysRevE.65.031206, 2002.

Choi, C. H. and Kim, C. J.: Large slip of aqueous liquid flow over a nanoengineered superhydrophobic surface, Physical Review Letters, 96, 066 001, doi:10.1103/PhysRevLett.96.066001, 2006.

Churaev, N. V., Sobolev, V. D., and Somov, A. N.: Slippage of liquids over lyophobic solid surfaces, Journal of Colloid And Interface Science, 97, 574–581, doi:10.1016/0021-9797(84)90330-8, 1984.

Claeys, M., Graham, B., Vas, G., Wang, W., Vermeylen, R., Pashynska, V., Cafmeyer, J., Guyon, P., Andreae, M. O., Artaxo, P., and Maenhaut, W.: Formation of secondary organic aerosols through photooxidation of isoprene, Science, 303, 1173–1176, doi:10.1126/science.1092805, 2004.

Collyer, A. A. and Clegg, D. W.: Rheological Measurement, Elsevier Applied Science Publishers Ltd, New York, NY, 1988.

Craig, V. S. J., Neto, C., and Williams, D. R. M.: Shear-dependent boundary slip in an aqueous Newtonian liquid, Physical Review Letters, 87, 054 504, doi:10.1103/PhysRevLett.87.054504, 2001.

Czechowski, G., Jarosiewicz, P., Rabiega, A., and Jadzyn, J.: The viscous properties of diols. IV. 1,2-and 1,4-butanediol in butanol solutions, Zeitschrift fur Naturforschung - Section A Journal of Physical Sciences, 59, 119–123, doi:10.1515/zna-2004-0304, 2004.

Ebben, C. J., Strick, B. F., Upshur, M. A., Chase, H. M., Achtyl, J. L., Thomson, R. J., and Geiger, F. M.: Towards the identification of molecular constituents associated with the surfaces of isoprene-derived secondary organic aerosol (SOA) particles, Atmospheric Chemistry and Physics, 14, 2303–2314, doi:10.5194/acp-14-2303-2014, 2014.

Edney, E. O., Kleindienst, T. E., Jaoui, M., Lewandowski, M., Offenberg, J. H., Wang, W., and Claeys, M.: Formation of 2-methyl tetrols and 2-methylglyceric acid in secondary organic aerosol from laboratory irradiated isoprene/NOX/SO2/air mixtures and their detection in ambient PM2.5 samples collected in the eastern United States, Atmospheric Environment, 39, 5281–5289, doi:10.1016/j.atmosenv.2005.05.031, 2005.

Först, P., Werner, F., and Delgado, A.: On the pressure dependence of the viscosity of aqueous sugar solutions, Rheologica Acta, 41, 369–374, doi:10.1007/s00397-002-0238-y, 2002.

Gao, S., Keywood, M. D., Ng, N. L., Surratt, J., Varutbangkul, V., Bahreini, R., Flagan, R. C., and Seinfeld, J. H.: Low-molecular-weight and oligomeric components in secondary organic aerosol from the ozonolysis of cycloalkenes and α-pinene, Journal of Physical Chemistry A, 108, 10 147–10 164, doi:10.1021/jp047466e, 2004.

Grayson, J. W., Song, M., Sellier, M., and Bertram, A. K.: Validation of the poke-flow technique combined with simulations of fluid flow for determining viscosities in samples with small volumes and high viscosities, Atmospheric Measurement Techniques, 8, 2463–2472, doi:10.5194/amt-8-2463-2015, 2015.

Grayson, J. W., Zhang, Y., Mutzel, A., Renbaum-Wolff, L., Böge, O., Kamal, S., Herrmann, H., Martin, S. T., and Bertram, A. K.: Effect of varying experimental conditions on the viscosity of α-pinene derived secondary organic material, Atmospheric Chemistry and Physics, 16, 6027–6040, doi:10.5194/acp-16-6027-2016, 2016.

Green, D. W. and Perry, R. H.: Perry's Chemical Engineers' Handbook, The McGraw-Hill Companies, New York, NY, 8 edn., 2007.

Guenther, A., Karl, T., Harley, P., Wiedinmyer, C., Palmer, P. I., and Geron, C.: Estimates of global terrestrial isoprene emissions using MEGAN (Model of Emissions of Gases and Aerosols from Nature), Atmospheric Chemistry and Physics, 6, 3181–3210, doi:10.5194/acpd-6-107-2006, 2006.

Hallquist, M., Wenger, J. C., Baltensperger, U., Rudich, Y., Simpson, D., Claeys, M., Dommen, J., Donahue, N. M., George, C., Goldstein, a. H., Hamilton, J. F., Herrmann, H., Hoffmann, T., Iinuma, Y., Jang, M., Jenkin, M. E., Jimenez, J. L., Kiendler-Scharr, A., Maenhaut, W., McFiggans, G., Mentel, T. F., Monod, A., Prévôt, a. S. H., Seinfeld, J. H., Surratt, J. D., Szmigielski, R., and Wildt, J.: The formation,

properties and impact of secondary organic aerosol: current and emerging issues, Atmospheric Chemistry and Physics, 9, 5155–5236, doi:10.5194/acp-9-5155-2009, 2009.

Hawkins, L. N., Baril, M. J., Sedehi, N., Galloway, M. M., De Haan, D. O., Schill, G. P., and Tolbert, M. A.: Formation of semisolid, oligomerized aqueous SOA: Lab simulations of cloud processing, Environmental Science and Technology, 48, 2273–2280, doi:10.1021/es4049626, 2014.

Haynes, W. M.: CRC Handbook of Chemistry and Physics, CRC Press/Taylor and Francis Group, Boca Raton, FL, 96 edn., 2015.

Hiemenz, P. C. and Lodge, T. P.: Polymer Chemistry, CRC Press, Boca Raton, FL, 2 edn., 2007.

Hinks, M. L., Brady, M. V., Lignell, H., Song, M., Grayson, J. W., Bertram, A., Lin, P., Laskin, A., Laskin, J., and Nizkorodov, S. A.: Effect of Viscosity on Photodegradation Rates in Complex Secondary Organic Aerosol Materials, Phys. Chem. Chem. Phys., 18, 8785–8793, doi:10.1039/C5CP05226B, http://pubs.rsc.org/en/Content/ArticleLanding/2015/CP/C5CP05226B, 2016.

Houle, F. A., Hinsberg, W. D., and Wilson, K. R.: Oxidation of a model alkane aerosol by OH radical: the emergent nature of reactive uptake, Phys. Chem. Chem. Phys., 17, 4412–4423, doi:10.1039/C4CP05093B, 2015.

Ignatius, K., Kristensen, T. B., Järvinen, E., Nichman, L., Fuchs, C., Gordon, H., Herenz, P., Hoyle, C. R., Duplissy, J., Garimella, S., Dias, A., Frege, C., Höppel, N., Tröstl, J., Wagner, R., Yan, C., Amorim, A., Baltensperger, U., Curtius, J., Donahue, N. M., Gallagher, M. W., Kirkby, J., Kulmala, M., Möhler, O., Saathoff, H., Schnaiter, M., Tomé, A., Virtanen, A., Worsnop, D., and Stratmann, F.: Heterogeneous ice nucleation of viscous secondary organic aerosol produced from ozonolysis of α-pinene, Atmospheric Chemistry and Physics Discussions, 15, 35 719–35 752, doi:10.5194/acpd-15-35719-2015, 2015.

Jarosiewicz, P., Czechowski, G., and Jadzyn, J.: The viscous properties of diols. V. 1,2-hexanediol in water and butanol solutions, Zeitschrift fur Naturforschung - Section A Journal of Physical Sciences, 59, 559–562, doi:10.1515/zna-2004-0905, 2004.

Jimenez, J. L., Canagaratna, M. R., Donahue, N. M., Prevot, A. S. H., Zhang, Q., Kroll, J. H., DeCarlo, P. F., Allan, J. D., Coe, H., Ng, N. L., Aiken, A. C., Docherty, K. S., Ulbrich, I. M., Grieshop, A. P., Robinson, A. L., Duplissy, J., Smith, J. D., Wilson, K. R., Lanz, V. A., Hueglin, C., Sun, Y. L., Tian, J., Laaksonen, A., Raatikainen, T., Rautiainen, J., Vaattovaara, P., Ehn, M., Kumala, M., Tomlinson, J. M., Collins, D. R., Cubison, M. J., Dunlea, E. J., Huffman, J. A., Onasch, T. B., Alfarra, M. R., Williams, P. I., Bower, K., Kondo, Y., Schneider, J., Drewnick, F., Borrmann, S., Weimer, S., Demerjian, K., Salcedo, D., Cottrell, L., Griffin, R., Takami, A., Miyoshi, T., Hatakeyama, S., Shimono, A., Sun, J. Y., Zhang, Y. M., Dzepina, K., Kimmel, J. R., Sueper, D., Jayne, J. T., Herndon, S. C., Trimborn, A. M., Williams, L. R., Wood, E. C., Middlebrook, A. M., Kolb, C. E., Baltensperger, U., and Worsnop, D. R.: Evolution of Organic Aerosols in the Atmosphere, Science, 326, 1525–1529, doi:10.1126/science.1180353, 2009.

Jin, B. J. and Padula, M.: Steady flows of compressible fluids in a rigid container with upper free boundary, Mathematische Annalen, 329, 723–770, doi:10.1007/s00208-004-0535-0, 2004.

Joly, L., Ybert, C., Bocquet, L., and Trizac, E.: Effets électrocinétiques sur surfaces glissantes, Houille Blanche, 1, 53–58, doi:10.1051/lhb:200601006, 2006.

Joseph, P. and Tabeling, P.: Direct measurement of the apparent slip length, Physical Review E - Statistical, Nonlinear, and Soft Matter Physics, 71, 035 303, doi:10.1103/PhysRevE.71.035303, 2005.

Kanakidou, M., Seinfeld, J. H., Pandis, S. N., Barnes, I., Dentener, F. J., Facchini, M. C., Van Dingenen, R., Ervens, B., Nenes, A., Nielsen, C. J., Swietlicki, E., Putaud, J. P., Balkanski, Y., Fuzzi, S., Horth, J., Moortgat, G. K., Winterhalter, R., Myhre, C. E. L., Tsigaridis, K., Vignati, E., Stephanou, E. G., and Wilson, J.: Organic aerosol and global climate modelling: a review, Atmospheric Chemistry and Physics, 5, 1053–1123, doi:10.5194/acp-5-1053-2005, 2005.

Kidd, C., Perraud, V., Wingen, L. M., and Finlayson-Pitts, B. J.: Integrating phase and composition of secondary organic aerosol from the ozonolysis of α-pinene., Proceedings of the National Academy of Sciences of the United States of America, 111, 7552–7557, doi:10.1073/pnas.1322558111, 2014.

Koop, T., Bookhold, J., Shiraiwa, M., and Pöschl, U.: Glass transition and phase state of organic compounds: dependency on molecular properties and implications for secondary organic aerosols in the atmosphere, Physical Chemistry Chemical Physics, 13, 19 238, doi:10.1039/c1cp22617g, 2011.

Kuwata, M. and Martin, S. T.: Phase of atmospheric secondary organic material affects its reactivity, doi:10.1073/pnas.1209071109, 2012.

Ladino, L. A., Zhou, S., Yakobi-Hancock, J. D., Aljawhary, D., and Abbatt, J. P. D.: Factors controlling the ice nucleating abilities of α-pinene SOA particles, Journal of Geophysical Research Atmospheres, 119, 9041–9051, doi:10.1002/2014JD021578, 2014.

Lambe, A. T., Chhabra, P. S., Onasch, T. B., Brune, W. H., Hunter, J. F., Kroll, J. H., Cummings, M. J., Brogan, J. F., Parmar, Y., Worsnop, D. R., Kolb, C. E., and Davidovits, P.: Effect of oxidant concentration, exposure time, and seed particles on secondary organic aerosol chemical composition and yield, Atmospheric Chemistry and Physics, 15, 3063–3075, doi:10.5194/acp-15-3063-2015, 2015.

Lee, J. Y. and Hildemann, L. M.: Surface tension of solutions containing dicarboxylic acids with ammonium sulfate, d-glucose, or humic acid, Journal of Aerosol Science, 64, 94–102, doi:10.1016/j.jaerosci.2013.06.004, 2013.

Li, Y. J., Liu, P., Gong, Z., Wang, Y., Bateman, A. P., Bergoend, C., Bertram, A. K., and Martin, S. T.: Chemical reactivity and liquid/nonliquid states of secondary organic material, Environmental Science and Technology, 49, 13 264–13 274, doi:10.1021/acs.est.5b03392, 2015.

Li, Z., D'eramo, L., Monti, F., Vayssade, A.-L., Chollet, B., Bresson, B., Tran, Y., Cloitre, M., and Tabeling, P.: Slip length measurements using µPIV and TIRF-based velocimetry, Israel Journal of Chemistry, 54, 1589–1601, doi:10.1002/ijch.201400111, http://doi.wiley.com/10.1002/ijch.201400111, 2014.

Lienhard, D. M., Huisman, A. J., Krieger, U. K., Rudich, Y., Marcolli, C., Luo, B. P., Bones, D. L., Reid, J. P., Lambe, A. T., Canagaratna, M. R., Davidovits, P., Onasch, T. B., Worsnop, D. R., Steimer, S. S., Koop, T., and Peter, T.: Viscous organic aerosol particles in the upper troposphere: Diffusivity-controlled water uptake and ice nucleation?, Atmospheric Chemistry and Physics, 15, 13 599–13 613, doi:10.5194/acp-15-13599-2015, 2015.

Lignell, H., Hinks, M. L., and Nizkorodov, S. A.: Exploring matrix effects on photochemistry of organic aerosols, Proceedings of the National Academy of Sciences, 111, 13 780–13 785, doi:10.1073/pnas.1322106111, 2014.

Lu, J. W., Rickards, A. M. J., Walker, J. S., Knox, K. J., Miles, R. E. H., Reid, J. P., and Signorell, R.: Timescales of water transport in viscous aerosol: measurements on sub-micron particles and dependence on conditioning history, Physical Chemistry Chemical Physics, 16, 9819–30, doi:10.1039/c3cp54233e, 2014.

MacDonald, G. A., Lanier, T. C., Swaisgood, H. E., and Hamann, D. D.: Mechanism for stabilization of fish actomyosin by sodium lactate, Journal of Agricultural and Food Chemistry, 44, 106–112, doi:10.1021/jf940698y, 1996.

Marrero-Morejón, J. and Pardillo-Fontdevila, E.: Estimation of liquid viscosity at ambient temperature of pure organic compounds by using group-interaction contributions, Chemical Engineering Journal, 79, 69–72, doi:10.1016/S1385-8947(99)00173-4, 2000.

Moller, B., Rarey, J., and Ramjugernath, D.: Estimation of the vapour pressure of non-electrolyte organic compounds via group contributions and group interactions, Journal of Molecular Liquids, 143, 52–63, doi:10.1016/j.molliq.2008.04.020, 2008.

Muller, L., Reinnig, M.-C., Hayen, H., and Hoffmann, T.: Characterization of oligomeric compounds in secondary organic aerosol using liquid chromatography coupled to electrospray ionization Fourier transform ion cyclotron resonance mass spectrometry, Rapid communications in mass spectrometry : RCM, 23, 971–979, doi:10.1002/rcm.3957, 2009.

Murray, B. J. and Bertram, A. K.: Inhibition of solute crystallisation in aqueous H(+)-NH(4)(+)-SO4(2-)-H2O droplets., Physical Chemistry Chemical Physics, 10, 3287–3301, doi:10.1039/b802216j, 2008.

Murray, B. J., Haddrell, A. E., Peppe, S., Davies, J. F., Reid, J. P., O'Sullivan, D., Price, H. C., Kumar, R., Saunders, R. W., Plane, J. M. C., Umo, N. S., and Wilson, T. W.: Glass formation and unusual hygroscopic growth of iodic acid solution droplets with relevance for iodine mediated particle formation in the marine boundary layer, Atmospheric Chemistry and Physics, 12, 8575–8587, doi:10.5194/acp-12-8575-2012, 2012.

Myrdal, P. B. and Yalkowsky, S. H.: Estimating pure component vapor pressures of complex organic molecules, Industrial & Engineering Chemistry Research, 36, 2494–2499, doi:10.1021/ie950242l, 1997.

Nannoolal, Y., Rarey, J., Ramjugernath, D., and Cordes, W.: Estimation of pure component properties: Part 1. Estimation of the normal boiling point of non-electrolyte organic compounds via group contributions and group interactions, Fluid Phase Equilibria, 226, 45–63, doi:10.1016/j.fluid.2004.09.001, 2004.

Nannoolal, Y., Rarey, J., and Ramjugernath, D.: Estimation of pure component properties: Part 3. Estimation of the vapor pressure of non-electrolyte organic compounds via group contribution and group interactions, Fluid Phase Equilibria, 269, 117–133, doi:10.1016/j.fluid.2008.04.020, 2008.

Neto, C., Evans, D. R., Bonaccurso, E., Butt, H.-J., and Craig, V. S. J.: Boundary slip in Newtonian liquids: a review of experimental studies, Reports on Progress in Physics, 68, 2859–2897, doi:10.1088/0034-4885/68/12/R05, 2005.

Nolte, C. G., Schauer, J. J., Cass, G. R., and Simoneit, B. R. T.: Highly polar organic compounds present in wood smoke and in the ambient atmosphere, Environmental Science and Technology, 35, 1912–1919, doi:10.1021/es001420r, 2001.

Pachaiyappan, V., Ibrahim, S. H., and Kuloor, N. R.: Simple correlation for determining viscosity of organic liquids, Chemical Engineering, p. 193, 1967.

Pajunoja, A., Malila, J., Hao, L., Joutsensaari, J., Lehtinen, K. E. J., and Virtanen, A.: Estimating the Viscosity Range of SOA Particles Based on Their Coalescence Time, Aerosol Science and Technology, 48, doi:10.1080/02786826.2013.870325, 2014.

Power, R. M., Simpson, S. H., Reid, J. P., and Hudson, A. J.: The transition from liquid to solid-like behaviour in ultrahigh viscosity aerosol particles, Chem. Sci., 4, 2597–2604, doi:10.1039/C3SC50682G, 2013.

Price, H. C., Murray, B. J., Mattsson, J., O'Sullivan, D., Wilson, T. W., Baustian, K. J., and Benning, L. G.: Quantifying water diffusion in high-viscosity and glassy aqueous solutions using a Raman isotope tracer method, Atmospheric Chemistry and Physics Discussions, 14, 3817–3830, doi:10.5194/acpd-13-29375-2013, 2014.

Price, H. C., Mattsson, J., Zhang, Y., Bertram, A. K., Davies, J. F., Grayson, J. W., Martin, S. T., O'Sullivan, D., Reid, J. P., Rickards, A. M. J., and Murray, B. J.: Water diffusion in atmospherically relevant α-pinene secondary organic material, Chemical Science, 6, 4876–4883, doi:10.1039/C5SC00685F, 2015.

Quintas, M., Brandão, T. R. S., Silva, C. L. M., and Cunha, R. L.: Rheology of supersaturated sucrose solutions, Journal of Food Engineering, 77, 844–852, doi:10.1016/j.jfoodeng.2005.08.011, 2006.

Renbaum-Wolff, L., Grayson, J. W., Bateman, A. P., Kuwata, M., Sellier, M., Murray, B. J., Shilling, J. E., Martin, S. T., and Bertram, A. K.: Viscosity of α-pinene secondary organic material and implications for particle growth and reactivity., Proceedings of the National Academy of Sciences of the United States of America, 110, 8014–8019, doi:10.1073/pnas.1219548110, 2013a.

Renbaum-Wolff, L., Grayson, J. W., and Bertram, A. K.: Technical Note: New methodology for measuring viscosities in small volumes characteristic of environmental chamber particle samples, Atmospheric Chemistry and Physics, 13, 791–802, doi:10.5194/acp-13-791-2013, 2013b.

Russell, L. M., Hawkins, L. N., Frossard, A. A., Quinn, P. K., Bates, T. S., and Finlayson-Pitts, B. J.: Carbohydrate-like composition of submicron atmospheric particles and their production from ocean bubble bursting, Proceedings of the National Academy of Sciences of the United States of America, 107, 6652–6657, doi:10.1073/pnas.0908905107, 2010.

Sastri, S. and Rao, K.: A new group contribution method for predicting viscosity of organic liquids, The Chemical Engineering Journal, 50, 9–25, doi:10.1016/0300-9467(92)80002-R, 1992.

Saukko, E., Lambe, A. T., Massoli, P., Koop, T., Wright, J. P., Croasdale, D. R., Pedernera, D. A., Onasch, T. B., Laaksonen, A., Davidovits, P., Worsnop, D. R., and Virtanen, A.: Humidity-dependent phase state of SOA particles from biogenic and anthropogenic precursors, Atmospheric Chemistry and Physics, 12, 7517–7529, doi:10.5194/acp-12-7517-2012, 2012.

Schill, G. P., O., D. H. D., and Tolbert, M. A.: Heterogeneous ice nucleation on simulated secondary organic aerosol, Environmental Science and Technology, 48, 1675–1692, doi:10.1021/es4046428, 2014.

Schnell, E.: Slippage of water over nonwettable surfaces, Journal of Applied Physics, 27, 1149–1152, doi:10.1063/1.1722220, 1956.

Sheely, M. L.: Glycerol viscosity tables, Industrial & Engineering Chemistry, 24, 1060–1064, doi:10.1021/ie50273a022, 1932.

Shiraiwa, M. and Seinfeld, J. H.: Equilibration timescale of atmospheric secondary organic aerosol partitioning, Geophysical Research Letters, 39, 1–6, doi:10.1029/2012GL054008, 2012.

Shiraiwa, M., Ammann, M., Koop, T., and Poschl, U.: Gas uptake and chemical aging of semisolid organic aerosol particles, Proceedings of the National Academy of Sciences of the United States of America, 108, 11 003–11 008, doi:10.1073/pnas.1103045108, 2011.

Shiraiwa, M., Zuend, A., Bertram, A. K., and Seinfeld, J. H.: Gas-particle partitioning of atmospheric aerosols: interplay of physical state, non-ideal mixing and morphology., Physical Chemistry Chemical Physics, 15, 11 441–11 453, doi:10.1039/c3cp51595h, 2013.

Sigma-Aldrich: 1,2,6-Hexanetriol, Tech. rep., Sigma-Aldrich, Milwaukee, WI, https://www.sigmaaldrich.com/content/dam/sigma-aldrich/docs/Aldrich/Bulletin/al{_}techbull{_}al128.pdf, 1996.

Song, M., Marcolli, C., Krieger, U. K., Zuend, A., and Peter, T.: Liquid-liquid phase separation and morphology of internally mixed dicarboxylic acids/ammonium sulfate/water particles, Atmospheric Chemistry and Physics, 12, 2691–2712, doi:10.5194/acp-12-2691-2012, 2012.

Song, M., Liu, P. F., Hanna, S. J., Li, Y. J., Martin, S. T., and Bertram, A. K.: Relative humidity-dependent viscosities of isoprene-derived secondary organic material and atmospheric implications for isoprene-dominant forests, Atmospheric Chemistry and Physics, 15, 5145–5159, doi:10.5194/acp-15-5145-2015, 2015.

Steimer, S. S., Berkemeier, T., Gilgen, A., Krieger, U. K., Peter, T., Shiraiwa, M., and Ammann, M.: Shikimic acid ozonolysis kinetics of the transition from liquid aqueous solution to highly viscous glass, Phys. Chem. Chem. Phys., 17, 31 101–31 109, doi:10.1039/C5CP04544D, 2015.

Stein, S. E. and Brown, R. L.: Estimation of normal boiling points from group contributions, Journal of Chemical Information and Computer Sciences, 34, 581–587, doi:10.1021/ci00019a016, 1994.

Stocker, T. F., Qin, D., Plattner, G.-K., Tignor, M. M. B., Allen, S. K., Boschung, J., Nauels, A., Xia, Y., Bex, V., and Midgely, P. M., eds.: IPCC Climate Change 2013: The Physical Science Basis. Contribution of Working Group I to the Fifth Assessment Report of the Intergovernmental Panel on Climate Change, Cambridge University Press, Cambridge, United Kingdom and New York, NY, USA, 2013.

Surratt, J. D., Murphy, S. M., Kroll, J. H., Ng, N. L., Hildebrandt, L., Sorooshian, A., Szmigielski, R., Vermeylen, R., Maenhaut, W., Claeys, M., Flagan, R. C., and Seinfeld, J. H.: Chemical composition of secondary organic aerosol formed from the photooxidation of isoprene, Journal of Physical Chemistry A, 110, 9665–9690, doi:10.1021/jp061734m, 2006.

Surratt, J. D., Chan, A. W., Eddingsaas, N. C., Chan, M., Loza, C. L., Kwan, a. J., Hersey, S. P., Flagan, R. C., Wennberg, P. O., and Seinfeld, J. H.: Reactive intermediates revealed in secondary organic aerosol formation from isoprene, Proceedings of the National Academy of Sciences of the United States of America, 107, 6640–6645, doi:10.1073/pnas.0911114107, 2010.

Swindells, J. F., Snyder, C. F., Hardy, R. C., and Golden, P. E.: Viscosities of sucrose solutions at various temperatures: Tables of recalculated values, Tech. rep., United States Department of Commerce, 1958.

Telis, V., Telis-Romero, J., Mazzotti, H., and Gabas, A.: Viscosity of aqueous carbohydrate solutions at different temperatures and concentrations, International Journal of Food Properties, 10, 185–195, doi:10.1080/10942910600673636, 2007.

Tolocka, M. P., Heaton, K. J., Dreyfus, M. A., Wang, S., Zordan, C. A., Saul, T. D., and Johnston, M. V.: Chemistry of particle inception and growth during α-pinene ozonolysis, Environmental Science and Technology, 40, 1843–1848, doi:10.1021/es051926f, 2006.

Tong, H. J., Reid, J. P., Bones, D. L., Luo, B. P., and Krieger, U. K.: Measurements of the timescales for the mass transfer of water in glassy aerosol at low relative humidity and ambient temperature, Atmospheric Chemistry and Physics, 11, 4739–4754, doi:10.5194/acp-11-4739-2011, 2011.

Tretheway, D. C. and Meinhart, C. D.: Apparent fluid slip at hydrophobic microchannel walls, Physics of Fluids, 14, doi:10.1063/1.1432696, 2002.

Upshur, M. A., Strick, B. F., McNeill, V. F., Thomson, R. J., and Geiger, F. M.: Climate-relevant physical properties of molecular constituents for isoprene-derived secondary organic aerosol material, Atmospheric Chemistry and Physics, 14, 10 731–10 740, doi:10.5194/acp-14-10731-2014, 2014.

Verevkin, S. P.: Determination of vapor pressures and enthalpies of vaporization of 1,2-alkanediols, Fluid Phase Equilibria, 224, 23–29, doi:10.1016/j.fluid.2004.05.010, 2004.

Virtanen, A., Joutsensaari, J., Koop, T., Kannosto, J., Yli-Pirilä, P., Leskinen, J., Mäkelä, J. M., Holopainen, J. K., Pöschl, U., Kulmala, M., Worsnop, D. R., and Laaksonen, A.: An amorphous solid state of biogenic secondary organic aerosol particles., Nature, 467, 824–827, doi:10.1038/nature09455, 2010.

Viswanath, D. S., Ghosh, T., Prasad, D. H. L., Dutt, N. V. K., and Rani, K. Y.: Viscosity of liquids, Springer, 2007.

Wang, B., Lambe, A. T., Massoli, P., Onasch, T. B., Davidovits, P., Worsnop, D. R., and Knopf, D. A.: The deposition ice nucleation and immersion freezing potential of amorphous secondary organic aerosol: Pathways for ice and mixed-phase cloud formation, Journal of Geophysical Research Atmospheres, 117, 1–12, doi:10.1029/2012JD018063, 2012.

Wang, B., O'brien, R. E., Kelly, S. T., Shilling, J. E., Moffet, R. C., Gilles, M. K., and Laskin, A.: Reactivity of liquid and semisolid secondary organic carbon with chloride and nitrate in atmospheric aerosols, Journal of Physical Chemistry A, 119, 4498–4508, doi:10.1021/jp510336q, 2015.

Watanabe, K., Udagawa, Y., and Udagawa, H.: Drag reduction of Newtonian fluid in a circular pipe with a highly water-repellent wall, Journal of Fluid Mechanics, 381, 225–238, doi:10.1017/S0022112098003747, 1999.

Wilson, T. W., Murray, B. J., Wagner, R., Möhler, O., Saathoff, H., Schnaiter, M., Skrotzki, J., Price, H. C., Malkin, T. L., Dobbie, S., and Al-Jumur, S. M. R. K.: Glassy aerosols with a range of compositions nucleate ice heterogeneously at cirrus temperatures, Atmospheric Chemistry and Physics, 12, 8611–8632, doi:10.5194/acp-12-8611-2012, 2012.

Worton, D. R., Surratt, J. D., Lafranchi, B. W., Chan, A. W. H., Zhao, Y., Weber, R. J., Park, J. H., Gilman, J. B., De Gouw, J., Park, C., Schade, G., Beaver, M., Clair, J. M. S., Crounse, J., Wennberg, P., Wolfe, G. M., Harrold, S., Thornton, J. A., Farmer, D. K., Docherty, K. S., Cubison, M. J., Jimenez, J. L., Frossard, A. A., Russell, L. M., Kristensen, K., Glasius, M., Mao, J., Ren, X., Brune, W., Browne,

E. C., Pusede, S. E., Cohen, R. C., Seinfeld, J. H., and Goldstein, A. H.: Observational insights into aerosol formation from isoprene, Environmental Science and Technology, 47, 11 403–11 413, doi:10.1021/es4011064, 2013.

Zaveri, R. A., Easter, R. C., Shilling, J. E., and Seinfeld, J. H.: Modeling kinetic partitioning of secondary organic aerosol and size distribution dynamics: Representing effects of volatility, phase state, and particle-phase reaction, Atmospheric Chemistry and Physics, 14, 5153–5181, doi:10.5194/acp-14-5153-2014, 2014.

Zelenyuk, A., Imre, D., Beránek, J., Abramson, E., Wilson, J., and Shrivastava, M.: Synergy between secondary organic aerosols and long-range transport of polycyclic aromatic hydrocarbons., Environmental Science & Technology, 46, 12 459–12 466, doi:10.1021/es302743z, 2012.

Zhang, X., McVay, R. C., Huang, D. D., Dalleska, N. F., Aumont, B., Flagan, R. C., and Seinfeld, J. H.: Formation and evolution of molecular products in α-pinene secondary organic aerosol., Proceedings of the National Academy of Sciences of the United States of America, 112, 14 168–14 173, doi:10.1073/pnas.1517742112, 2015.

Zhou, S., Lee, a. K. Y., McWhinney, R. D., and Abbatt, J. P. D.: Burial effects of organic coatings on the heterogeneous reactivity of particle-borne benzo[a]pyrene (BaP) toward ozone, Journal of Physical Chemistry A, 116, 7050–7056, doi:10.1021/jp3030705, 2012.

Zhou, S., Shiraiwa, M., McWhinney, R. D., Pöschl, U., and Abbatt, J. P. D.: Kinetic limitations in gas-particle reactions arising from slow diffusion in secondary organic aerosol, Faraday Discussions, 165, 391, doi:10.1039/c3fd00030c, 2013.

Zhu, L., Neto, C., and Attard, P.: Reliable measurements of interfacial slip by colloid probe atomic force microscopy. III. Shear-rate-dependent slip, Langmuir, 28, 3465–3473, doi:10.1021/la204566h, 2012.

Zobrist, B., Marcolli, C., Pedernera, D. A., and Koop, T.: Do atmospheric aerosols form glasses?, Atmospheric Chemistry and Physics, 8, 5221–5244, doi:10.5194/acpd-8-9263-2008, 2008.

Atmos. Chem. Phys. Discuss., doi:10.5194/acp-2016-672, 2016
Manuscript under review for journal Atmos. Chem. Phys.
Published: 4 August 2016

Atmospheric Chemistry and Physics Discussions

Figures and Tables

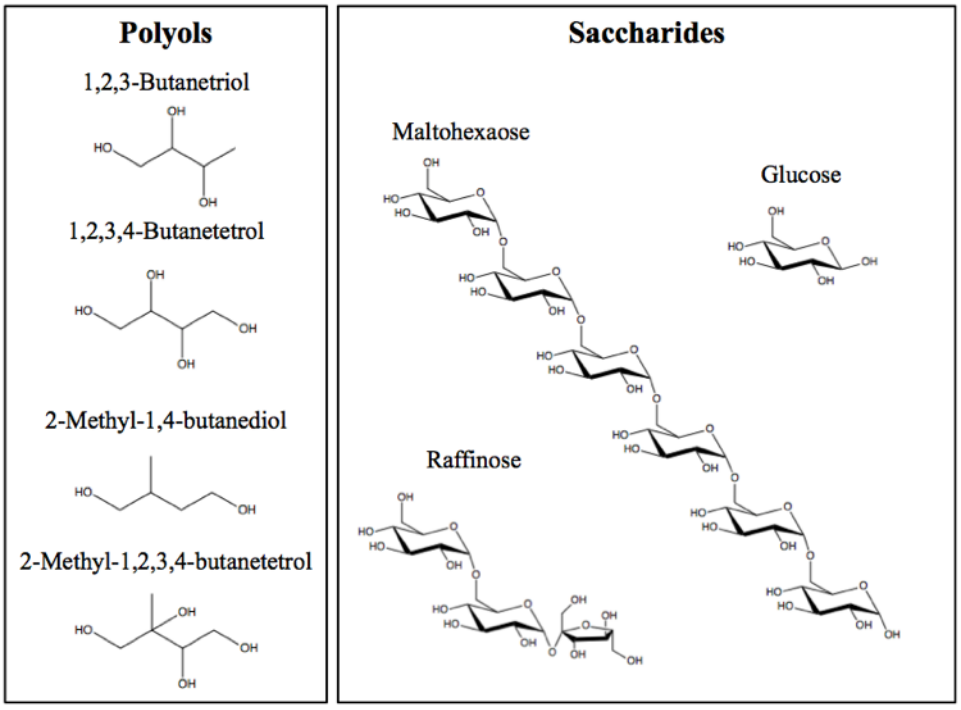

Figure 1. The structure of the polyols and saccharides studied experimentally in this work.

Atmos. Chem. Phys. Discuss., doi:10.5194/acp-2016-672, 2016
Manuscript under review for journal Atmos. Chem. Phys.
Published: 4 August 2016

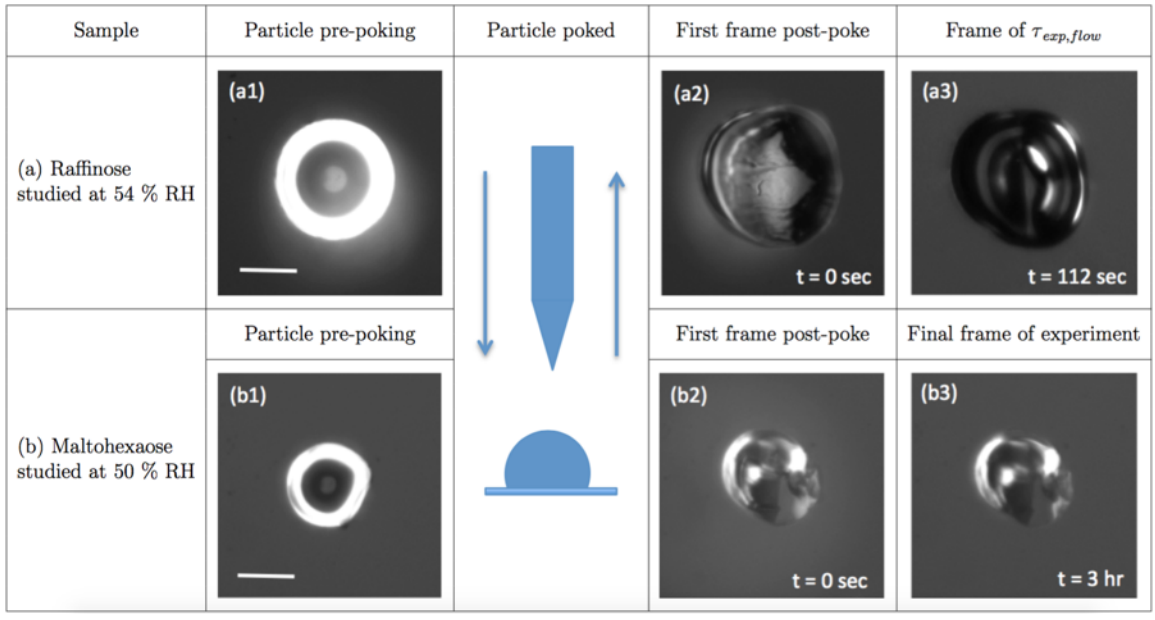

Figure 2. Optical images recorded during poke-and-flow experiments using particles of a) raffinose-water and b) maltohexaose-water mixtures. Images a1 and b1 correspond to the particles prior to being poked, with the white haloes being an optical effect. Images a2 and b2 correspond to the first frame after the needle has been removed. The particle comprised of raffinose and studied at 54 % RH exhibited flow, and image a3 corresponds to an image of the particle at its experimental flow time, $\tau_{exp,flow}$, the point at which the diameter of the hole at the centre of the torus has decreased to 50 % of its original size. The particle composed of maltohexaose and studied at 50 % RH exhibited cracking behaviour and, as shown in image b3, no change in the size or shape of the cracks can be observed 3 h after the particle has been poked. The scale bars in images a1 and b1 correspond to 20 μm.

Atmos. Chem. Phys. Discuss., doi:10.5194/acp-2016-672, 2016
Manuscript under review for journal Atmos. Chem. Phys.
Published: 4 August 2016

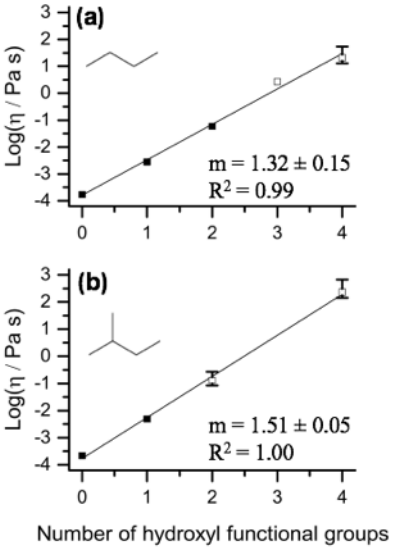

Figure 3. A plot of log(viscosity / Pa s) vs. the number of OH functional groups for (a) linear C4 and (b) branched C5 carbon backbones. Literature values (Czechowski et al., 2004; Haynes, 2015; Viswanath et al., 2007) are represented using filled symbols, and values measured experimentally in this study are represented using open symbols. Each solid line is a linear fit to the data in the panel, and values of the slope (m) are reported at the bottom right corner of the relevant plot, along with the corresponding coefficient of determination (R^2). The structures of the relevant carbon backbones are shown in the top left corner of each plot.

Atmos. Chem. Phys. Discuss., doi:10.5194/acp-2016-672, 2016
Manuscript under review for journal Atmos. Chem. Phys.
Published: 4 August 2016

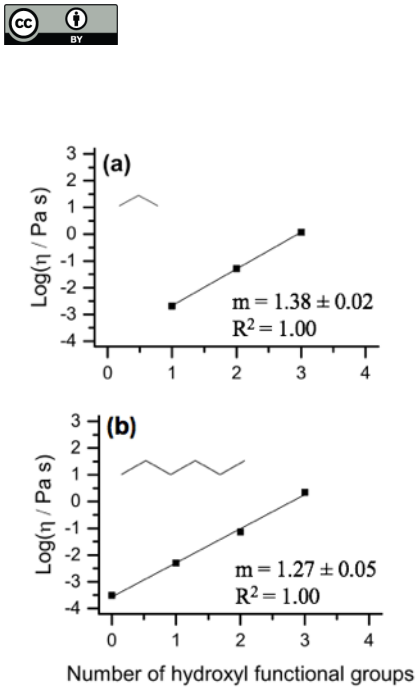

Figure 4. A plot of log(viscosity / Pa s) vs. the number of OH functional groups for (a) linear C3 and (b) linear C6 carbon backbones using literature values (Czechowski et al., 2004; Haynes, 2015; Sheely, 1932; Sigma-Aldrich, n.d.). Each solid line is a linear fit to the data in the panel, and values of the slope (m) are reported at the bottom right corner of the relevant plot, along with the corresponding coefficient of determination (R^2). The structures of the relevant carbon backbones are shown in the top left corner of each plot.

Atmos. Chem. Phys. Discuss., doi:10.5194/acp-2016-672, 2016
Manuscript under review for journal Atmos. Chem. Phys.
Published: 4 August 2016

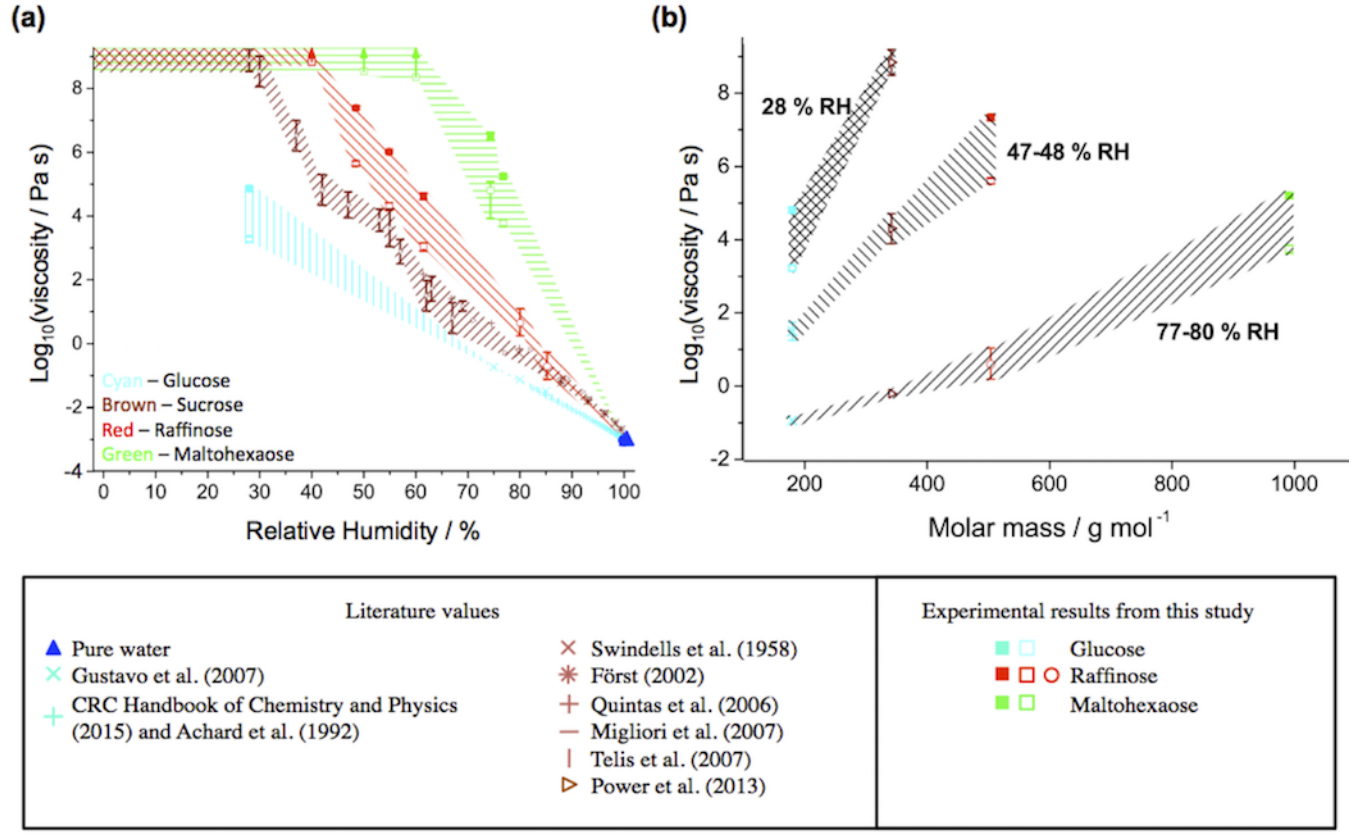

Figure 5. Plots of $\log_{10}$(viscosity) vs. (a) relative humidity and (b) molar mass for glucose, sucrose, raffinose, and maltohexaose. Values determined experimentally here were measured at 294-295 K. Results determined in the current study using the bead-mobility technique are shown using circle symbols, and those determined using the poke-and-flow technique are shown using squares, with filled squares representing upper limits of viscosity and open squares representing lower limits of viscosity, with y-error bars representing 95 % confidence intervals for both techniques, as detailed in Table 4. Also included are literature viscosity values (measured at 293 or 298 K) for sucrose (Först et al., 2002; Power et al., 2013; Quintas et al., 2006; Swindells et al., 1958; Telis et al., 2007) and glucose (Achard et al., 1992; Barbosa-Canovas, 2007; Haynes, 2015). The viscosity of glucose at 47 % shown in (b) was determined using a polynomial fit to the data shown in (a). The viscosity of water is also added to (a). Shaded regions are added to (a) and (b) to guide the readers eye.

Atmos. Chem. Phys. Discuss., doi:10.5194/acp-2016-672, 2016
Manuscript under review for journal Atmos. Chem. Phys.
Published: 4 August 2016

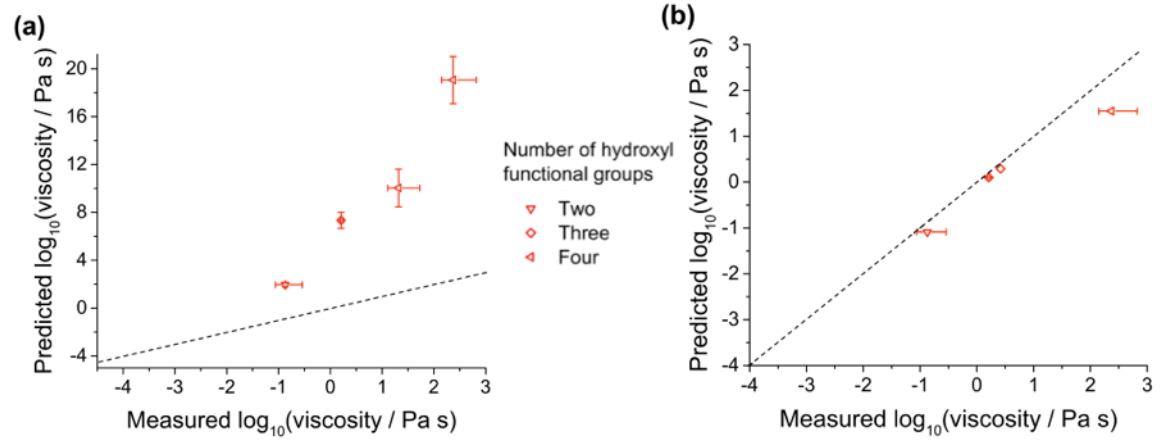

Figure 6. Plot of measured vs.predicted $\log_{10}$(viscosity) for the polyols measured in the current study: 2-methyl-1,4-butanediol, 1,2,3-butanetriol, 2-methyl-1,2,3,4-butanetetrol, and 1,2,3,4-butanetetrol. a) Predictions using the model of Sastri and Rao (1992) and b) predictions using the model of Marrero-Morejon and Padillo-Fontdevila (2000). Dashed 1:1 lines are shown on each plot. Error bars on the x-axis represent uncertainty in viscosities for compounds measured experimentally here, whilst error bars on the y-axis observed in (a) are due to the range of predicted vapour pressures using the QSPR models discussed in the text.

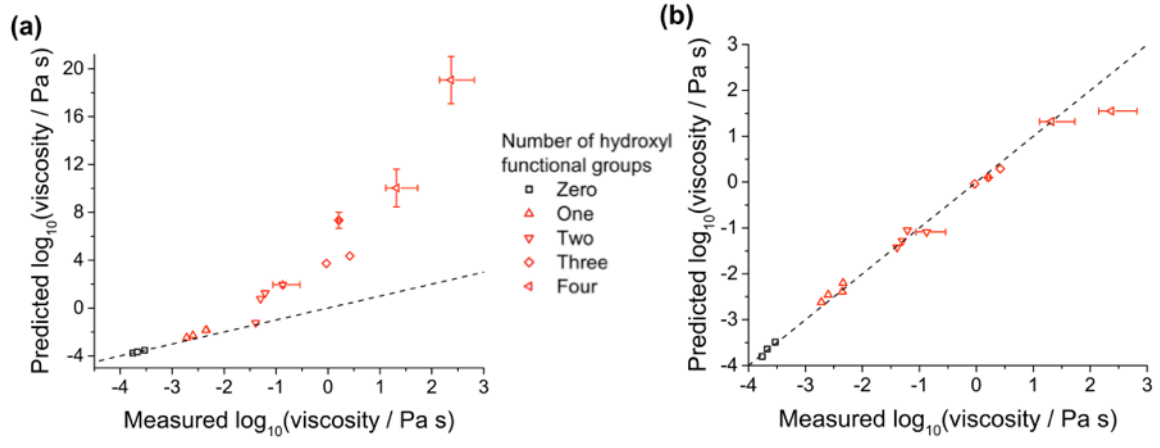

Figure 7. Plot of measured vs. predicted $\log_{10}$(viscosity) of C3-C6 alkanes, alcohols, and polyols. a) Predictions using the model of Sastri and Rao (1992) and b) predictions using the model of Marrero-Morejon and Padillo-Fontdevila (2000). In this figure measured data includes that taken from literature. Dashed 1:1 lines are shown on each plot. Error bars on the x-axis represent uncertainty in viscosities for compounds measured experimentally here, whilst error bars on the y-axis observed in (a) are due to the range of predicted vapour pressures using the QSPR models discussed in the text.

Atmos. Chem. Phys. Discuss., doi:10.5194/acp-2016-672, 2016
Manuscript under review for journal Atmos. Chem. Phys.
Published: 4 August 2016

Atmospheric Chemistry and Physics Discussions

Table 1. Properties of polyol and saccharide compounds studied experimentally.

Compound	Chemical formula	O:C	Molar mass (g mol^{-1})
2-Methyl-1,4-butanediol	$C_5H_{12}O_2$	0.40	104
1,2,3-Butanetriol	$C_4H_{10}O_3$	0.75	106
1,2,3,4-Butanetetrol	$C_4H_{10}O_4$	1.00	122
2-Methyl-1,2,3,4-butanetetrol	$C_5H_{12}O_4$	0.80	136
Glucose	$C_6H_{12}O_6$	1.00	180
Raffinose	$C_{18}H_{32}O_{16}$	0.89	504
Maltohexaose	$C_{36}H_{62}O_{31}$	0.86	991

Table 2. Physical parameters used in the COMSOL Multiphysics simulations for cases where flow was observed in the poke-and-flow experiments. R and r indicate the radius of a tube and the radius of an inner hole, respectively, of the half-torus geometry used in the simulations.

		Slip length (nm)	Surface tension (mN m^{-1})	Density (g cm^{-3})	Contact angle (°)[a]
Glucose	Lower limit	5[b]	72.0[c]	1.0[d]	66 (if r < 2R), 73 (if r>2R)
	Upper limit	10,000[b]	95.1[e]	1.7[f]	73 (if r < 2R), 66 (if r > 2R)
Raffinose	Lower limit	5[b]	72.0[c]	1.0 [d]	58 (if r < 2R), 67 (if r >2R)
	Upper limit	10,000[b]	125.8[e]	1.9[f]	67 (if r < 2R), 58 (if r >2R)
Maltohexaose	Lower limit	5[b]	72.0[c]	1.0 [d]	63 (if r < 2R), 73 (if r > 2R)
	Upper limit	10,000[b]	138.2[e]	2.0[f]	73 (if r < 2R), 63 (if r > 2R)

[a] Contact angles were determined from optical images of millimeter sized droplets deposited on hydrophobic substrates. Millimeter sized droplets were deposited onto hydrophobic substrates and allowed to equilibrate for 30 minutes. Then digital photographs were taken. Contact angles at the particle-substrate interface were determined from the acquired images using ImageJ software.

[b] This slip length range is based on experimental measurements of the slip length for organic-water compounds on hydrophobic surfaces (Baudry et al., 2001; Cheng and Giordano, 2002; Choi and Kim, 2006; Churaev et al., 1984; Craig et al., 2001; Jin and Padula, 2004; Joly et al., 2006; Joseph and Tabeling, 2005; Li et al., 2014; Neto et al., 2005; Schnell, 1956; Tretheway and Meinhart, 2002; Watanabe et al., 1999; Zhu et al., 2012).

[c] The lower limit of the surface tension used in the simulations corresponds to the surface tension of pure water at 293 K. Experimental measurements have determined glucose-water and sucrose-water solutions at 293 K to have a greater surface tension than that of pure water (Lee and Hildemann, 2013; MacDonald et al., 1996). It is assumed that the same is true for raffinose-water and maltohexaose-water solutions.

[d] The lower limit of density corresponds to the density of water.

[e] For upper limits to the surface tension of saccharide-water solutions we use the surface tensions predicted for each of the pure saccharides by ACD/Labs. Values obtained from www.chemspider.com.

[f] The upper limits of density for glucose, raffinose, and maltohexaose are the upper limits of density predicted for each of the pure compounds by ACD/Labs. Values obtained from www.chemspider.com.

Atmos. Chem. Phys. Discuss., doi:10.5194/acp-2016-672, 2016
Manuscript under review for journal Atmos. Chem. Phys.
Published: 4 August 2016

Atmospheric Chemistry and Physics Discussions

Table 3. Physical parameters used to simulate a lower limit of viscosity for poke-and-flow experiments where particles were observed to crack when impacted by the needle, and no observable flow of material was observed over the course of the experiment.

Slip length (nm)	Surface tension (mN m^{-1})	Density (g cm^{-3})	Contact angle (°)
10-17[a]	72.0[b]	1.8[c]	90[d]

[a] In the simulations a slip length of 0.01*k was used, where k is the grid spacing of the mesh used in the simulation. Since a grid spacing of 1 to 1.7 μm was used in the simulations, the slip length ranged from 10 nm to 17 nm. Further details are available in Renbaum-Wolff et al. (2013b).

[b] The surface tension corresponds to the surface tension of pure water at 293 K, which is the estimated lower limit of surface tension for raffinose-water and maltohexaose-water solutions. The viscosity determined in simulations increases with surface tension, so the lower limit of surface tension gives rise to the simulated lower limit of viscosity.

[c] The predicted densities of raffinose and maltohexaose based on ACD/Labs are 1.8±0.1 and 1.9±0.1 g cm^{-3}, respectively.

[d] In cases where particles cracked and did not flow, the calculated lower limit of viscosity is independent of the contact angle between 20° and 100° (Renbaum-Wolff et al., 2013b). For the current study we used a contact angle of 90°, which falls within this range.

Table 4. Measured viscosities for the polyol and the saccharide-water mixtures studied here, with results from individual particles grouped by RH. The error associated with the rotational rheometer was not available, and so an error of 5 % has been used, greater than the stated error of 0.1 % reported for a similar rotational rheometer (Viscotester 550, Haake, Austria). For experiments using the bead-mobility technique, the mean is reported along with the 95 % confidence intervals. For experiments using the poke-and-flow technique, lower and upper limits of viscosity are reported, taking account of the 95 % confidence limits of the simulated lower and upper limits of viscosity for the group of particles studied at each RH. N/A represents not applicable.

Compound	Relative humidity (%)	Viscosity measurements			
		Technique	Mean	Lower limit	Upper limit
2-Methyl-1,4-butanediol	<0.5	Bead-mobility	1.3e-1	8.7e-2	2.9e-1
1,2,3-Butanetriol	<0.5	Rotational rheometer	1.6e0	1.5e0	1.7e0
1,2,3,4-Butanetetrol	<0.5	Bead-mobility	2.1e1	1.3e1	5.5e1
2-Methyl-1,2,3,4-butanetetrol	<0.5	Bead-mobility	2.3e2	1.4e2	6.5e2
Glucose	28	Poke-and-flow	N/A	1.3e3	7.7e4
Raffinose	85	Bead-mobility	1.9e-1	0.8e-1	5.2e-1
	80	Bead-mobility	4.3e0	1.7e0	1.2e1
	61	Poke-and-flow	N/A	7.4e2	4.7e4
	55	Poke-and-flow	N/A	1.4e4	1.0e6
	48	Poke-and-flow	N/A	3.4e5	2.4e7
	40	Poke-and-flow	N/A	6.0e8	N/A
Maltohexaose	77	Poke-and-flow	N/A	4.3e3	1.9e5
	74	Poke-and-flow	N/A	7.6e3	3.7e6
	60	Poke-and-flow	N/A	4.0e8	N/A
	50	Poke-and-flow	N/A	3.0e8	N/A